

**Military Technical College  
Kobry El-Kobbah,  
Cairo, Egypt**



**6<sup>th</sup> International Conference  
on Electrical Engineering  
ICEENG 2008**

## **MICROPROCESSOR CONTROL OF BRUSHLESS DC MOTOR**

*By*

S.A.Gawish \*

R. M. Mostafa \*\*

F. A. Khalifa \*\*\*

### **Abstract:**

This work focuses on investigation and evaluation of the performance of a permanent magnet brushless dc motor (BLDCM) drive, controlled by PID or fuzzy logic control techniques. The mathematical models of brushless DC motor with sinusoidal back EMF supplied from three-phase inverter operating at 180° conduction mode, and that with trapezoidal back EMF supplied from three-phase inverter operating at 120° conduction mode are given. In the simulation part the mathematical models are transferred to simulink models for PID and fuzzy logic control techniques. The gate driving simulink models for each control technique and for each mode of operation are designed and implemented. The system speed responses under the influence of load changes and set speed changes are presented. The three-phase currents, voltages, and electrical torque waveforms are presented. An experimental setup was constructed and tested. It consists of BLDCM, inverter, DC generator with variable resistive load and two personal computers. The load is automatically changed during operation by switching on and off relay contacts controlled by microprocessor. The fuzzy or PID control algorithms are implemented in one of the used personal computers while the other computer is used for data logging via a data acquisition card. In this study the system performance with PID controller and fuzzy controller is investigated and tested to achieve speed control under different loads and set speeds.

---

\* Modern Academy, Maadi, Cairo, Egypt

\*\* Beni-Suif University, Beni-Suif, Egypt

\*\*\* Suez-Canal University, Suez, Egypt

## 1. INTRODUCTION

The term “brushless dc motor” is used to identify a particular type of self-synchronous permanent magnet motor. In this motor the combination of ac machine, solid state inverter and rotor position sensor results in a drive system having a linear torque-speed characteristics, as in conventional dc machine. The permanent magnet synchronous machine has a polyphase winding on the stator and permanent magnets on the rotor. It must be supplied from a source ( the inverter ) the frequency of which always corresponds to the speed of its rotor [5,6].

Motor operation is made self-synchronous by the addition of a rotor position sensor that controls the firing signals of the solid state inverter. In response to these firing signals; the inverter directs current through the stator phase windings in a controlled sequence. The position sensors detect the position of the rotor poles and send control signals to switch on and off the devices in the dc-ac inverter at a frequency corresponding to the rotor speed.

## 2. MATHEMATICAL MODELING OF BLDCM

The BLDCM has three windings on the stator and permanent magnets on the rotor. Since both the magnet and the stainless-steel retaining sleeves have high resistivity, rotor-induced currents can be neglected and no damper windings are modeled. Hence the circuit equations of the three windings in phase variables are[3,4]:

$$\begin{bmatrix} v_a \\ v_b \\ v_c \end{bmatrix} = \begin{bmatrix} R & 0 & 0 \\ 0 & R & 0 \\ 0 & 0 & R \end{bmatrix} \begin{bmatrix} i_a \\ i_b \\ i_c \end{bmatrix} + \frac{d}{dt} \begin{bmatrix} L_a & L_{ba} & L_{ca} \\ L_{ba} & L_b & L_{bc} \\ L_{ca} & L_{bc} & L_c \end{bmatrix} \begin{bmatrix} i_a \\ i_b \\ i_c \end{bmatrix} + \begin{bmatrix} e_a \\ e_b \\ e_c \end{bmatrix} \quad (1)$$

Where :

$v_a, v_b, v_c$  : The applied stator voltages ;

$i_a, i_b, i_c$ : The stator currents;

$R$  : Stator resistance per phase ;

$L_a, L_b, L_c$  : The self inductances of the stator windings,

$L_{ab}, L_{bc}, L_{ca}$  : The mutual inductances of the stator windings,

$e_a, e_b, e_c$  : the induced EMFs in the stator windings

Assuming further that there is no change in the rotor reluctances with angle  $\theta$  [3,4], then

:  $L_a = L_b = L_c = L$  and  $L_{ab} = L_{bc} = L_{ca} = M$   
 And since  $i_a + i_b + i_c = 0$  then (1) will be

$$\begin{bmatrix} v_a \\ v_b \\ v_c \end{bmatrix} = \begin{bmatrix} R & 0 & 0 \\ 0 & R & 0 \\ 0 & 0 & R \end{bmatrix} \begin{bmatrix} i_a \\ i_b \\ i_c \end{bmatrix} + \frac{d}{dt} \begin{bmatrix} L-M & 0 & 0 \\ 0 & L-M & 0 \\ 0 & 0 & L-M \end{bmatrix} \begin{bmatrix} i_a \\ i_b \\ i_c \end{bmatrix} + \begin{bmatrix} e_a \\ e_b \\ e_c \end{bmatrix} \quad (2)$$

The electromagnetic torque will be given by:

$$T_e = (e_a i_a + e_b i_b + e_c i_c) / \omega_r \quad (3)$$

And the equation of motion is

$$\frac{2}{P} * J \frac{d\omega_r}{dt} = \left( T_e - T_L - \frac{2}{P} * B_m \omega_r \right) \quad (4)$$

Where:

$\omega_r$  : The electrical rotor angular velocity

J : the inertia of motor,

$B_m$ : the damping coefficient,

$T_L$  : the load torque,

P : the number of poles.

$\theta_m$  : the mechanical angular position of rotor.

## 2.1 Simulink Bldcm Model With Trapezoidal Emf

The general equations (1) to (4) are written in S-domain to describe the mathematical model of BLDCM with trapezoidal emf as follows:

$$I_a = \frac{V_a - E_a}{R + S(L - M)} \quad (5)$$

$$I_b = \frac{V_b - E_b}{R + S(L - M)} \quad (6)$$

$$I_c = \frac{V_c - E_c}{R + S(L - M)} \quad (7)$$

$$\omega_r = \frac{P}{2} (T_e - T_L) \left( \frac{1}{JS + B_m} \right) \quad (8)$$

Figure 1 shows the block diagram of BLDCM with trapezoidal back EMF. In this model the trapezoidal function of position is obtained from sinusoidal function by a limiter. This block diagram is converted into the simulink model given in figure 2 by taking into consideration of the motor parameters.

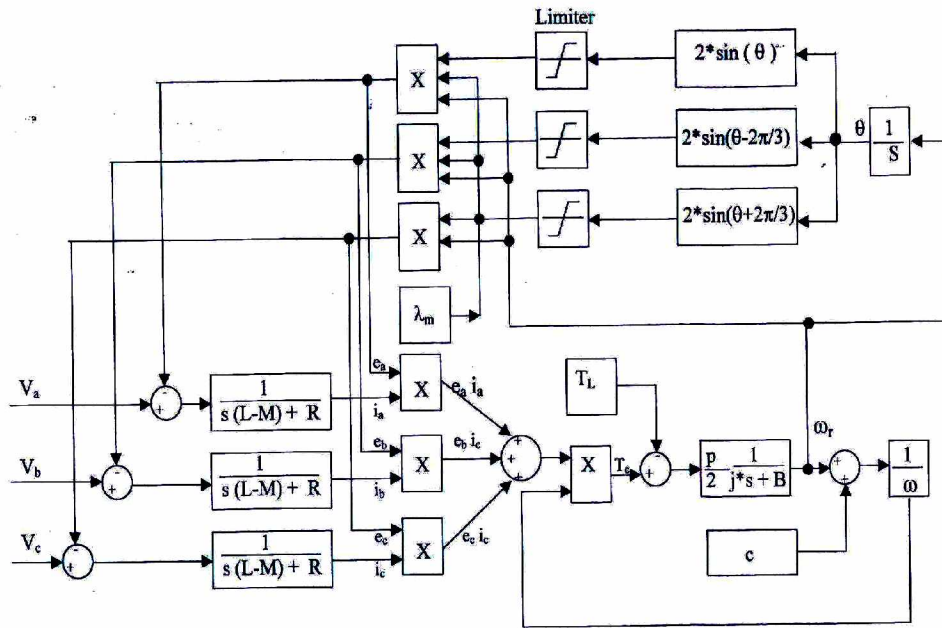


Fig (1) Block daigram of BLDCM with trapezoidal back

## 2.2 Model Of BLDCM With Sinusoidal Back EMF

The brushless dc motor considered is a three phase permanent magnet synchronous motor with a sinusoidal back EMF. The stator windings are identical, displaced by  $120^\circ$  and sinusoidally distributed. The model is obtained from equations (1) to (4) by writing the sinusoidal EMF equations as follows:

where :  $\theta_r$  = The electrical rotor angular displacement.,  
 $\lambda_m$  = The amplitude of the flux linkage

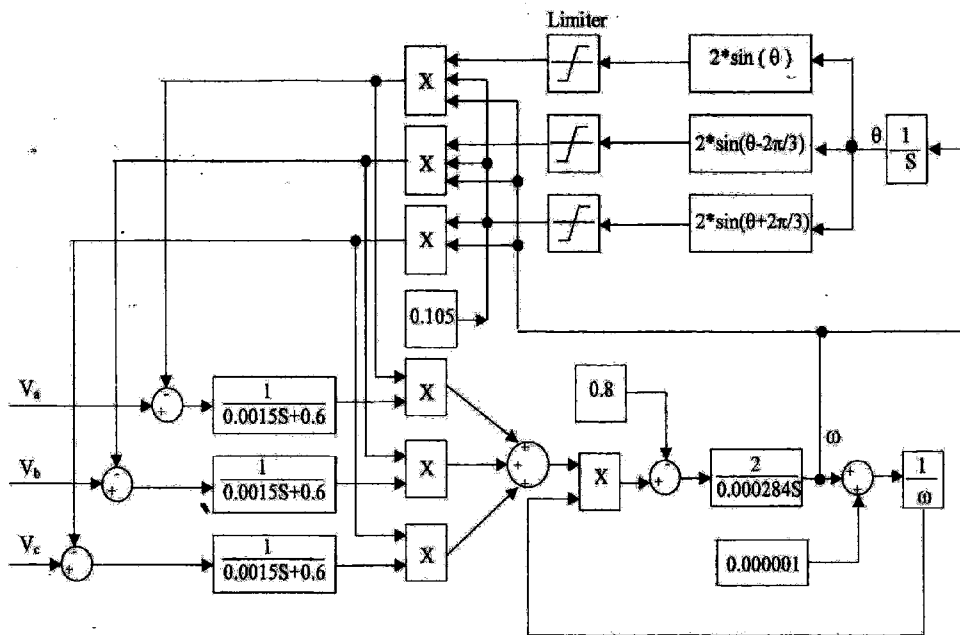


Fig. (2) Simulink model of BLDCM with trapezoidal EMF

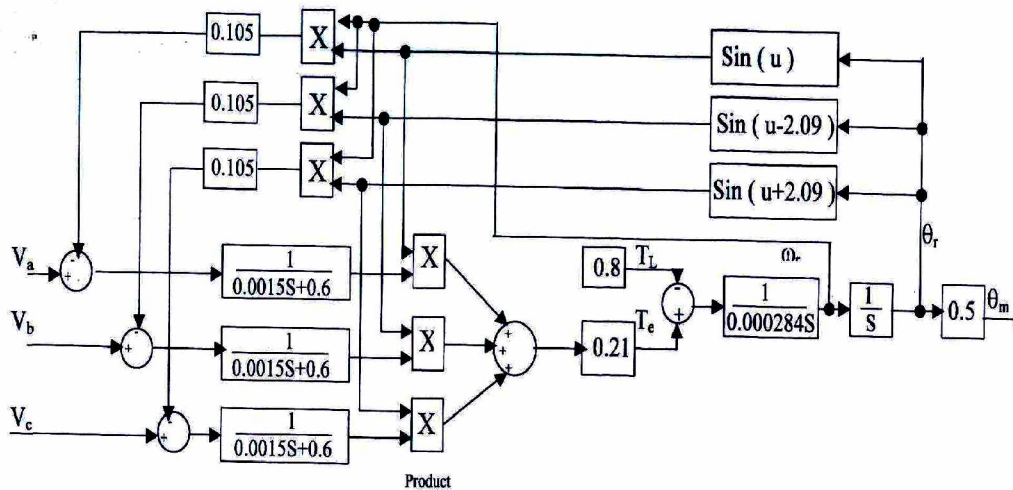


Fig. (3) Simulink model of BLDCM with sinusoidal EMF

The electromagnetic torque will be expressed as

$$T_e = \frac{P\lambda_m}{2} [(i_a \sin(\theta_r) + i_b \sin(\theta_r - 2\pi/3) + i_c \sin(\theta_r + 2\pi/3))] \quad (10)$$

$$\theta_r = \int \omega_r dt \quad (11)$$

$$\theta_m = \frac{2}{p} \theta_r \quad (12)$$

The simulink model of figure(3) can be constructed using equations (5) to (12) and the motor parameters (  $p = 4$ ,  $R = 0.5 \Omega$ ,  $\lambda_m = 0.105$ ,  $L-M = 0.0015$ ,  $B_m = 0$ ).  $T_L$  is replaced by a constant source.

### 3. THREE-PHASE INVERTER MODEL

#### 3.1.1 Inverter

A three-phase output can be obtained from configuration of six transistors and six diodes as shown in figure(4).

The gating signals of three phase inverters should be advanced or delayed by  $120^\circ$  with respect to each other in order to obtain three-phase balanced voltages. There are two types of control signals that can be applied to the transistors:  $180^\circ$  conduction or  $120^\circ$  conduction.

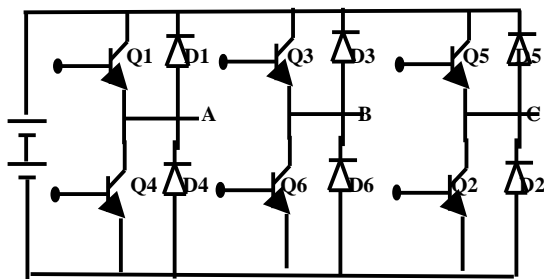


Fig. (4) Three phase inverter

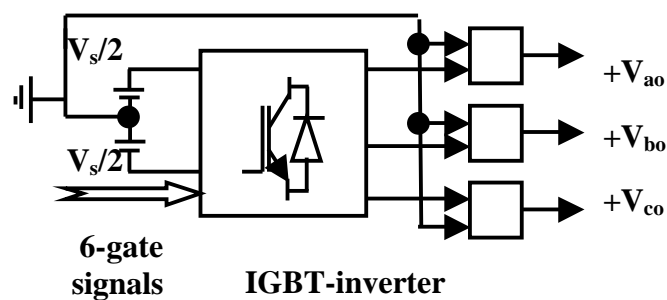


Fig (5) Simulink inverter model

The simulink model of the three phase inverter is obtained using the toolbox of MATLAB as: IGBT inverter, Voltage source, and Output voltage reference: ( the mid-point of the source voltage is considered as the reference point for the output phase voltages). This is shown by the summing block in figure (5)

### 3.1.2 Gate Signal Generation In Simulink

#### a- Sinusoidal Emfs

The 6-gate signals in SIMULINK are generated as follows ( see figure 6 ) :

Three sinusoidal signals  $\sin\theta_r$ ,  $\sin(\theta_r-2\pi/3)$ , and  $\sin(\theta_r+2\pi/3)$  are generated using sin function blocks. These 3 functions are multiplied by the controller output to obtain sinusoidal functions with controllable amplitudes according to the fuzzy or PID controller output. The frequency depends on rotor position .The generated sine waves are then compared with sawtooth signals with constant amplitude and frequency in order to obtain pulse width modulated signals.

#### b- Trapezoidal EMFs

The sinusoidal functions  $\sin\theta_r$ ,  $\sin(\theta_r-2\pi/3)$ , and  $\sin(\theta_r+2\pi/3)$  are generated using sin function blocks as before. Each function is multiplied by 2 and then using limiter to generate trapezoidal functions with unity amplitude. These functions are then multiplied by the controller output in order to obtain trapezoidal functions with controlled amplitudes . The generated trapezoidal waves are then compared with triangular signals with constant amplitude and frequency in order to obtain pulse width modulated signals. The frequency of the trapezoidal signals determines the number of pulses in each half cycle. This is called trapezoidal modulation. Each trapezoidal wave generates two gate signals for the two transistors in the same arm in order to prevent their switching on at the same instance. In our simulink model, the triangular wave frequency =10KHz, and the amplitude is 1 volt, as shown in figure(7).

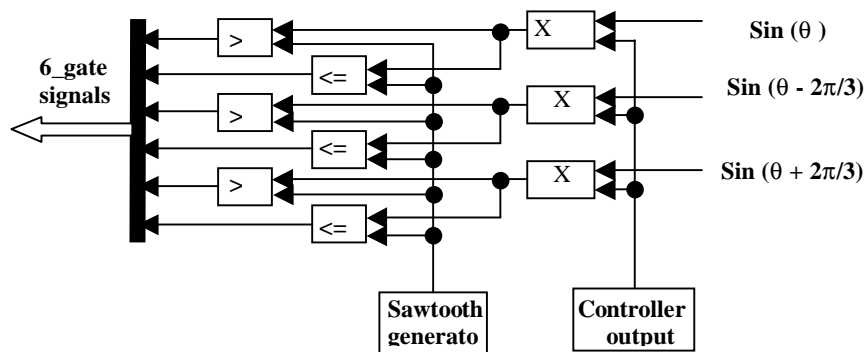


Fig (6) Simulink gate signal generation for sinusoidal EMF

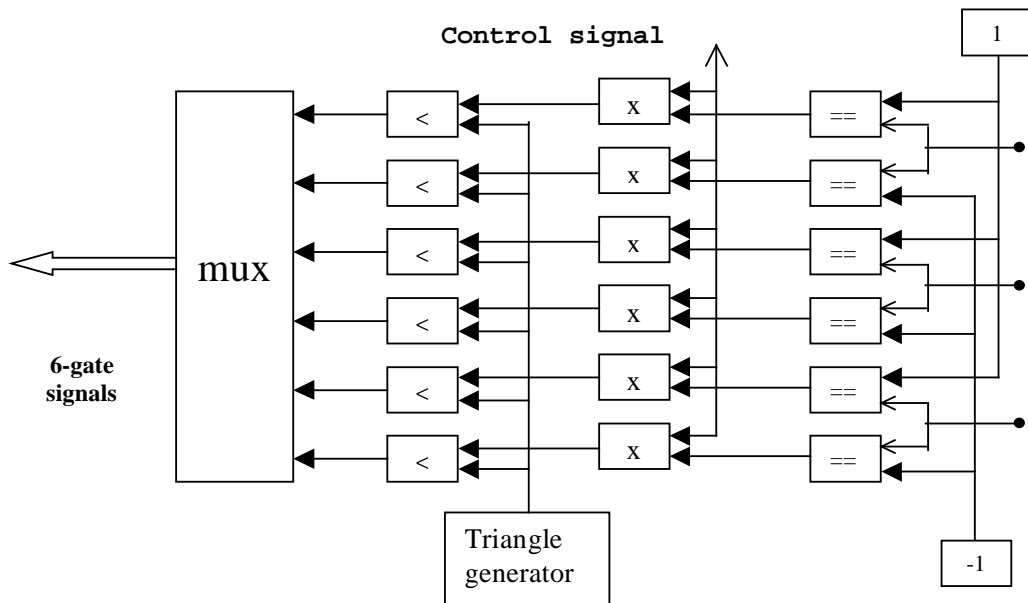


Fig.(7) Simulink model for trapezoidal EMF

#### 4. CONTROLLER SIMULINK MODEL

##### a-Fuzzy Controller

In order to construct the fuzzy controller simulink model, the fuzzy inference system file (FIS) is created first. It is the main part of the fuzzy model because it contains the normalized membership functions for each input and output as well as the rule base system between inputs and output. The number of these rules depends on the number of membership functions of each input. In this work 7 membership functions are chosen for each of the error input, the change of error input and the fuzzy output as shown in figure (8). Figure (9), shows the fuzzy controller simulink model.

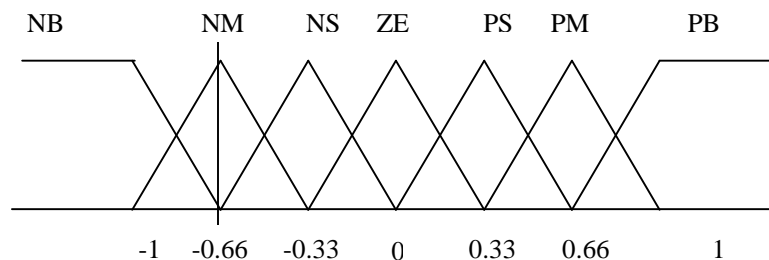


Fig. (8) Membership function

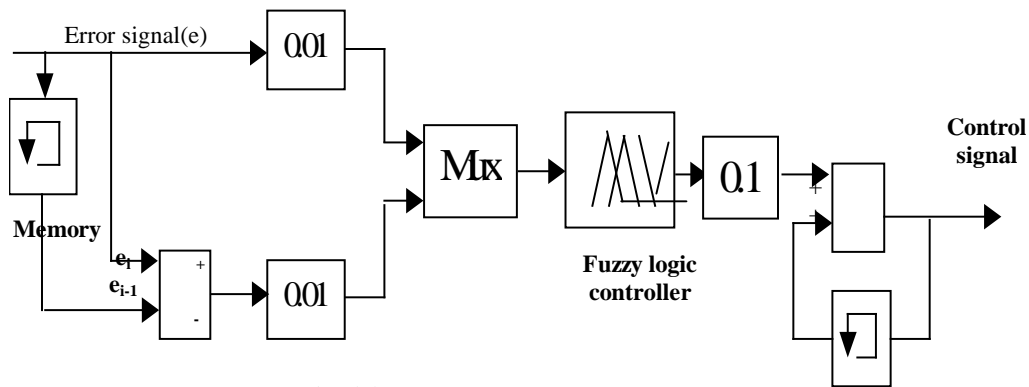


Fig (9) Fuzzy control model

### b-PID Controller

The simulink model of PID controller is shown in fig.10

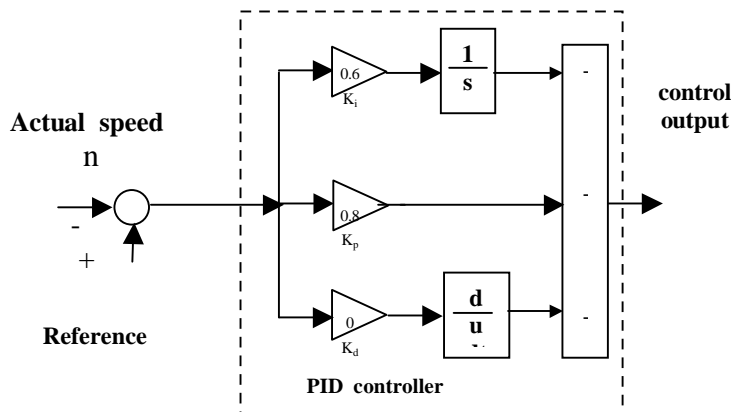


Fig (10) Simulink PID controller model

The complete simulink model of the system with fuzzy controller or PID controller is shown in figure (11).

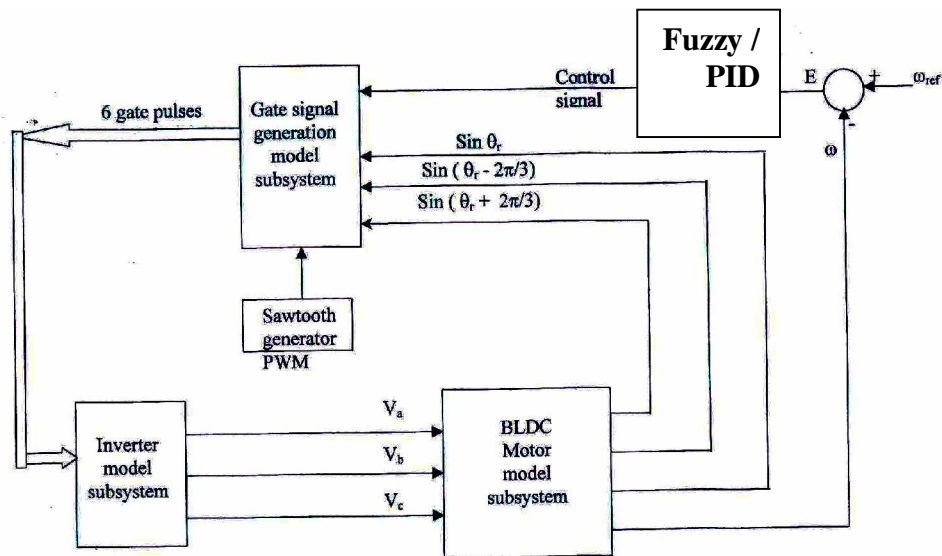
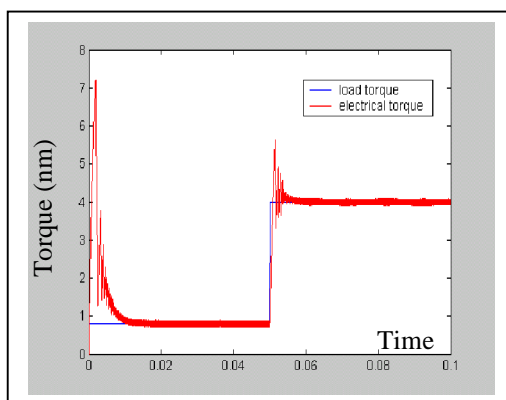


Fig (11) Complete system Simulink model

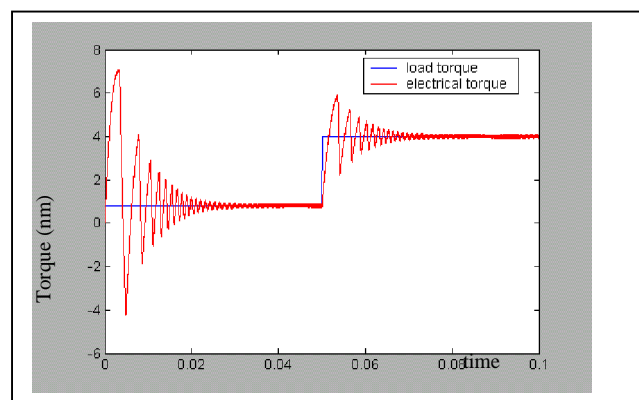
## 5. SIMULATION RESULTS

### a-BLDCM WITH SINUSOIDAL EMF

Figures 12 to 16 show the electromagnetic torque ,speed , three phase armature currents and pulse width modulated line voltage using PID controller and fuzzy logic controller for BLDCM with sinusoidal emf .The system behaviour is studied from starting to steady state and also when the load torque is changed after 0.05 second from the instant of starting. We chose a sampling time of 1  $\mu$  sec in simulation process ( $T_s=1 \mu s$ ). Figures 16 shows the speed response when the reference speed is changed

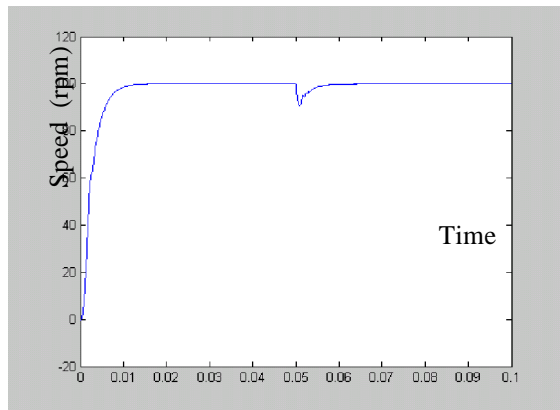


a-PID controller

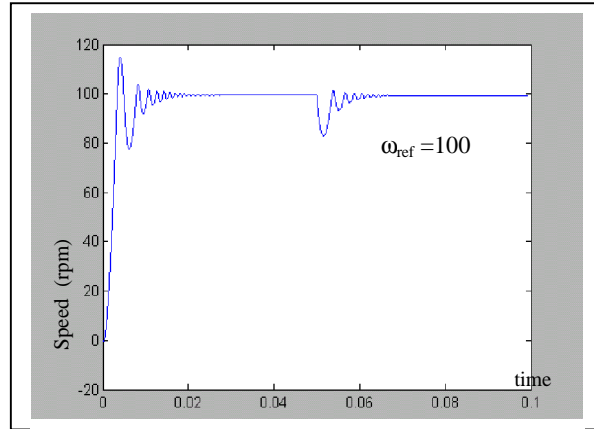


b- Fuzzy controller

Figure (12) the electromagnetic torque response to load change

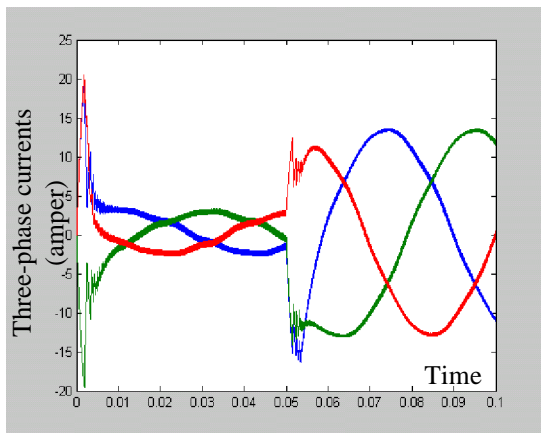


**a- PID controller**

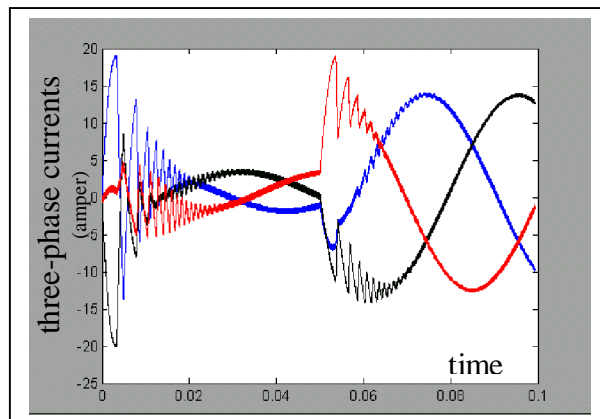


**b-Fuzzy controller**

**Figure (13) the speed response to load change**

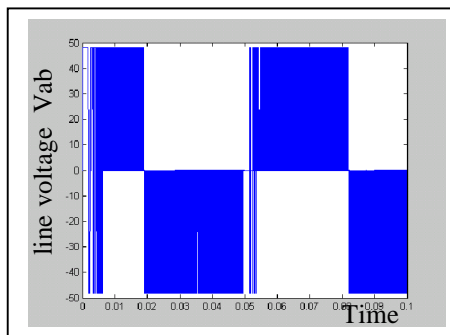


**a-PID controller**

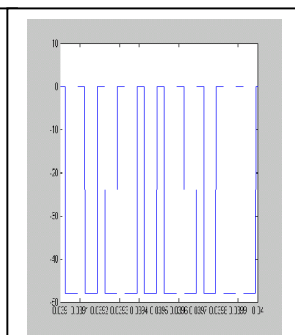


**b-Fuzzy controller**

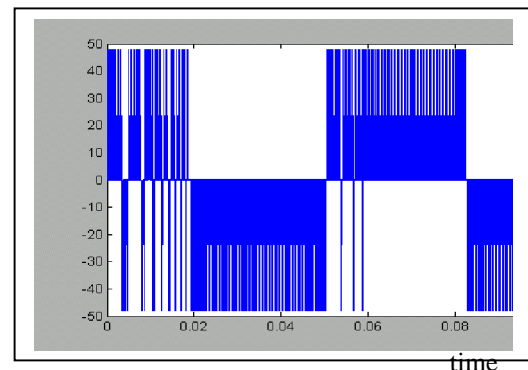
**Figure (14) the three-phase armature currents.**



**V<sub>ah</sub> waveform**



**Zooming at 0.04 sec**



**b-Fuzzy controller**

**a-PID controller**

**Fig (15) Line voltage Vab**

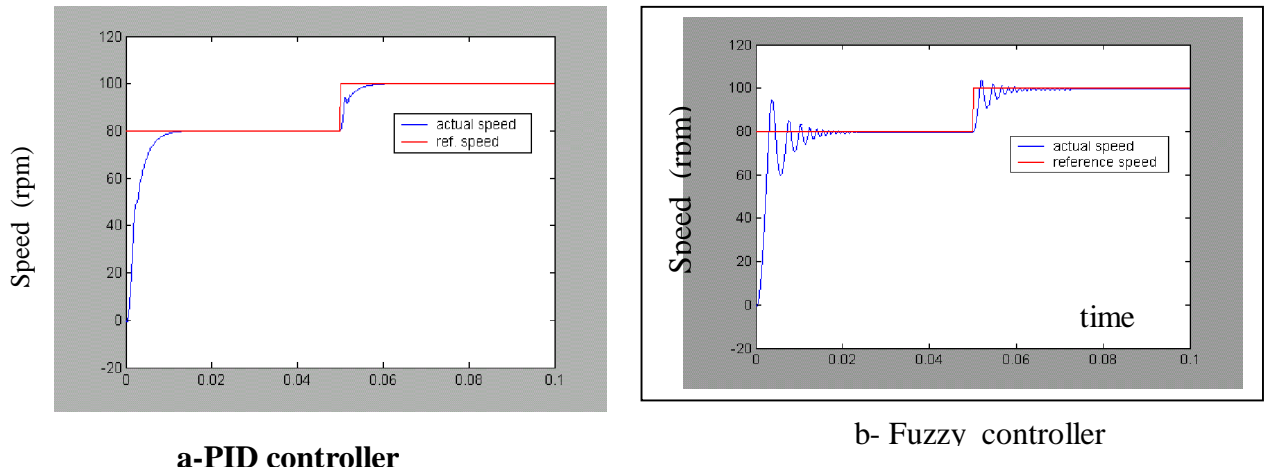


**Figure 16** Speed response due to change in reference speed by 20 rpm

The system with PID controller has fast response without overshoot and with no steady state error. while the system with fuzzy controller has damped oscillations and fastly reaches the reference speed

**b-Bldcm With Trapezoidal Emf And 120° ConductionUsing PID Controller**

The following results are taken for BLDCM model with trapezoidal emf and 120 degree conduction mode using PID controller.

Figure (17) shows the three-phase currents without load disturbance. Figure (18) shows the line voltage Vab at 100 rpm reference speed.

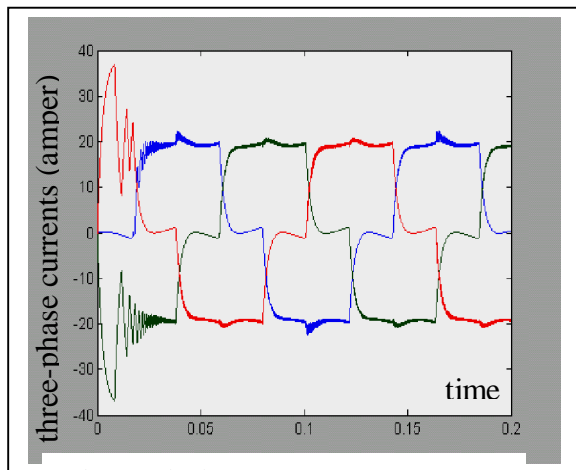


**Figure (17)** three-phase currents without load disturbance

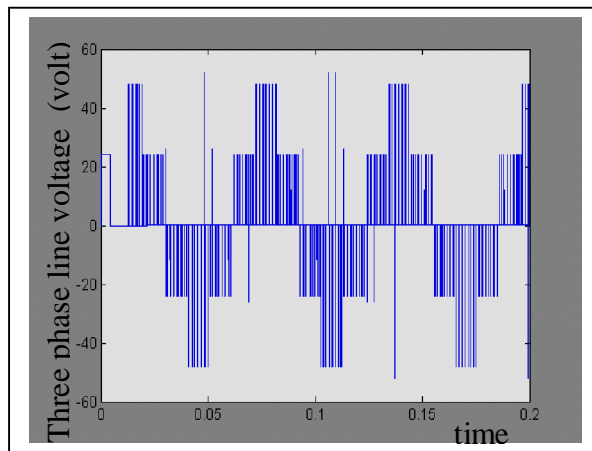


**Figure (18)** the line voltage at  $\omega_{ref}=100$  rpm

Figure(19) displays the effect of load torque change on three-phase currents .  
 Figure (20) shows the angular speed response to load change

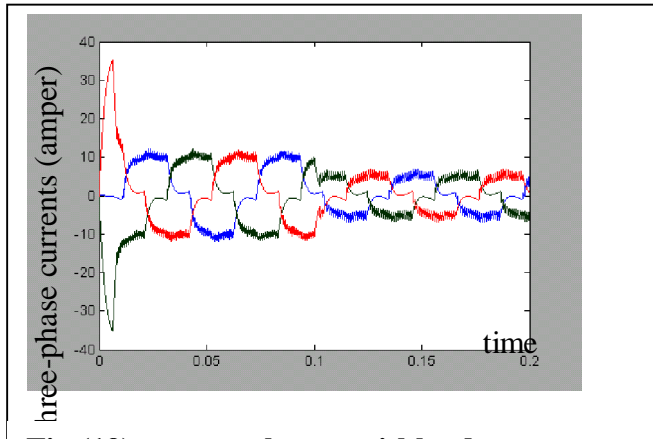


Fig (19) current change withload torque

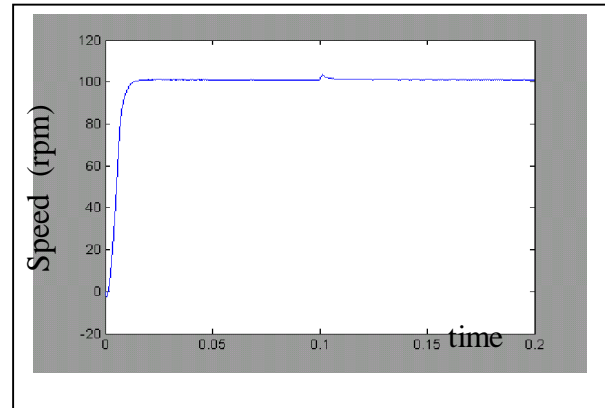


Figure (20) speed response to load change

## 6. PRACTICAL IMPLEMENTATION

An experimental setup (figure 21) was constructed and tested. It consists

- BLDCM with three phase IGBT inverter and position sensor.
- DC generator (mechanical load) with different resistive loads automatically selectable by microprocessor during operation via relay circuit.
- Personal computer in which Matlab package with real time operation capability exists
- Data acquisition card PCL-818 with eight differential analog input channels and two analog output channels.
- Tacho generator for speed feedback and speed response detection.
- Another personal computer for data logging.

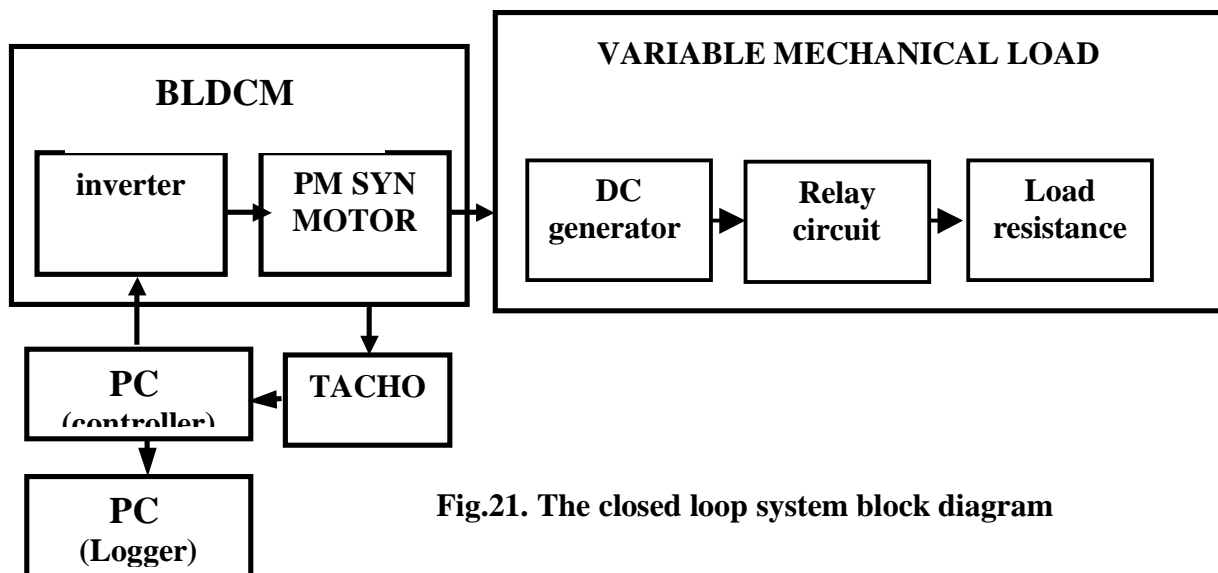


Fig.21. The closed loop system block diagram

The fuzzy or PID control algorithms are implemented in one of the computers using SIMULINK. The speed is sensed by the tacho generator, filtered and connected to A/D channel of the PCL-818 card and then to the input of the controller. The digital controller output is changed to analog value through one of the PCL-818 output channels and connected to the gate firing circuit of the IGBT inverter. The digital speed is also transferred to the other computer for data logging.

The system is started from rest at certain mechanical load. The load is automatically increased after 15 sec and then returned to initial value after another 15 sec. Finally the system will automatically stop after a third 15 sec. The logged speed file will be opened to trace the speed response. The speed response due to change in reference speed is also given.

### 6.1 Closed loop system with PID controller

the closed loop system with PID controller is shown in figure (22). The sampling time is chosen to be  $T_s = 0.4$  ms. The system was tested at different combinations of proportional, integral, and differential gains  $K_p$ ,  $K_I$ , and  $K_D$  respectively. A satisfactory performance is obtained when:

$$K_p = 0.8, K_I = 0.6, \text{ and } K_D = 0.0001$$

The system response is shown in figure 23 –25

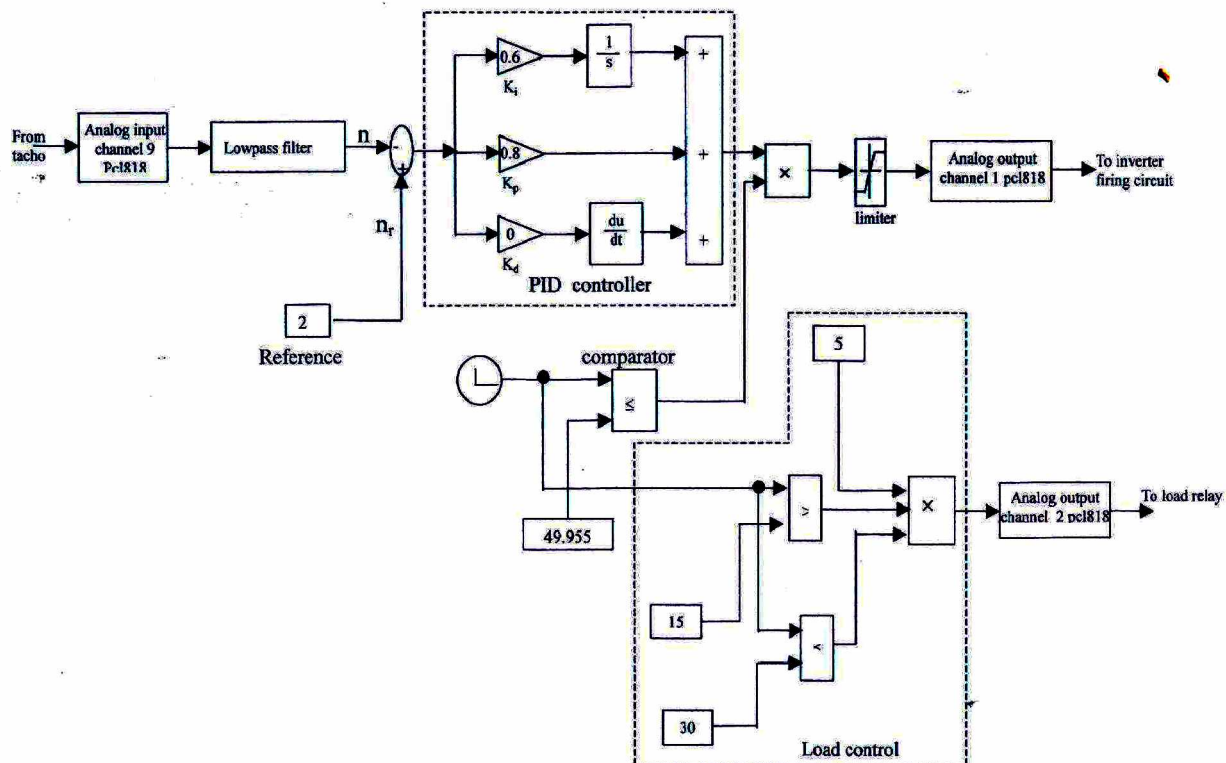


Figure (22): feedback system block diagram with PID controller

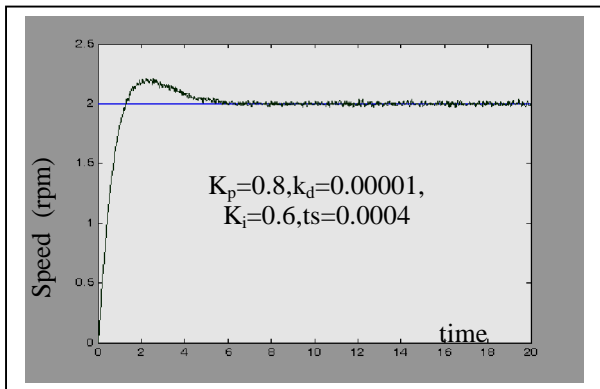


Fig (23) Response of the system without load

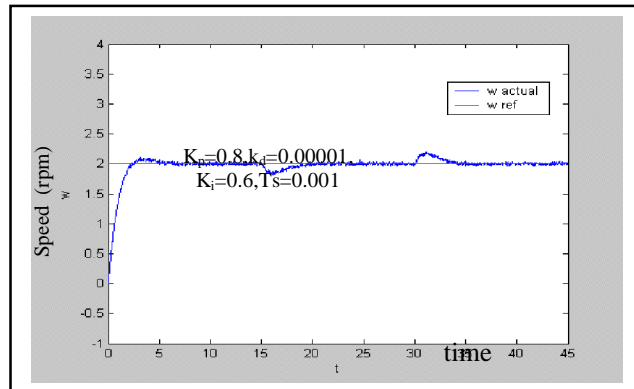


Fig (24) Speed response at different loads

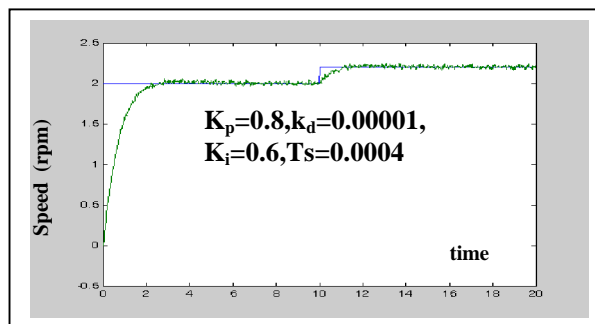


Fig (24) Speed response for reference speed change (200rpm)

## 6.2 Closed loop system with fuzzy controller

the closed loop system with **fuzzy** controller is shown in figure (25). The sampling time is chosen to be  $T_s = 2 \text{ ms}$ . The inputs to the fuzzy controller are the speed error  $e$  and the change of error  $\Delta e$ . The error gain  $K_e$  is chosen to have two values. A smaller value  $K_{e1}$  is chosen at starting because the error itself is big due to wide difference between the reference speed and the actual speed. When the error  $e$  becomes small by the controller action another gain  $K_{e2} > K_{e1}$  is suggested. It was also found that applying the same technique to the change of error gain  $K_{ce}$  has slight effect. Thus a single value is chosen for  $K_{ce}$ . In the other hand choosing two different values  $K_1$  and  $K_2$  for the fuzzy output gain improved greatly the speed response.

The normalized error and change of error were limited to be within the range  $\pm 1$ . This was achieved by using linear function with saturation as shown in figure(9).

The parameters used are:

$K_{e1}$  : Error gain at starting time,  $K_{e2}$  : Error gain after starting time,

$K_{ce}$  : Change of error gain

$K_1$  : Output gain at starting time,  $K_2$  : Output gain after starting time

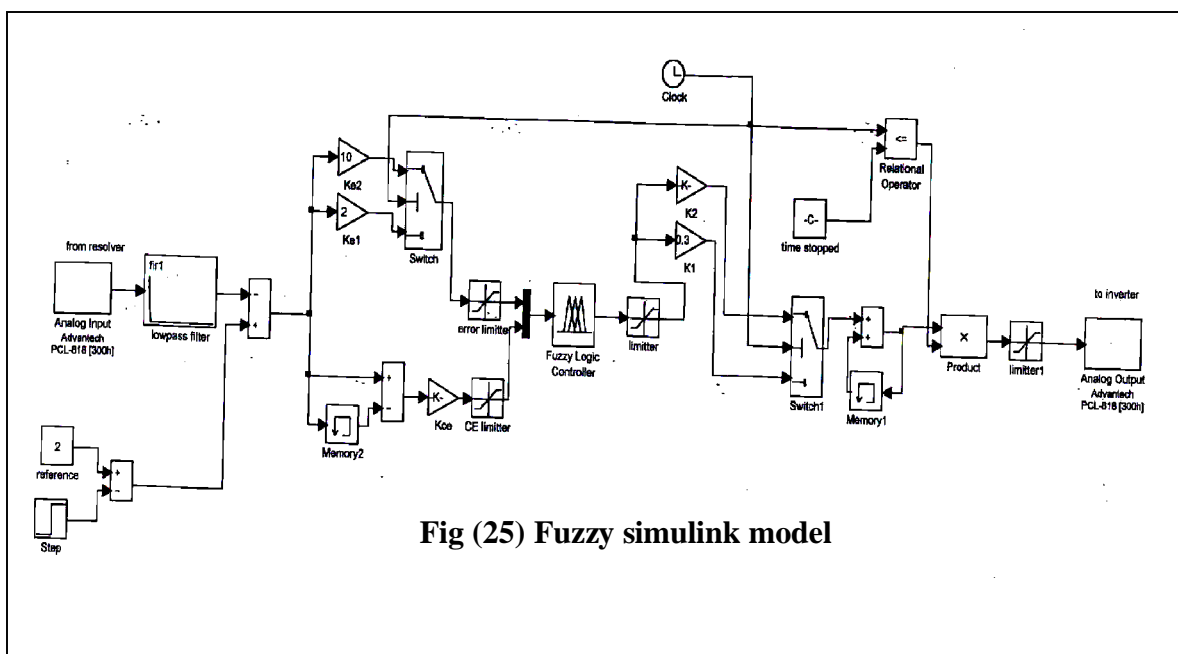
The simulink switch has three inputs, (input1, control input, and input3). The output of this switch is equals to input1 if the control input is less than the switching preset value, while it is equal to input2 if the input value is greater than the preset value.

The two fuzzy normalized input signals (e & ce) are multiplexed to the input of fuzzy logic controller simulink block. This block uses fuzzy inference system (FIS) file to perform FLC steps. The FIS file contains the membership functions for error, change of error and the output. It contains the fuzzy logic rules (49 rules corresponding to the 7 fuzzy sets for each input). The rules are in the form:

If e is NB and ce is NB then output u is NVB

The normalized output of the fuzzy controller is multiplied by the gain ( $k_1=0.3$ ) or ( $K_2=0.001$ ) to give the actual additive value to the control signal  $\Delta u(t)$ . The output of the sum3 ( $u(t)$ ) is given by  $u(t)=\Delta u(t)+u(t-1)$ . The control signal is reduced to zero after certain time elapse in order to stop the motor operation. The most suitable gains of the FLC obtained after several trials are:

$K_{e1}$	$K_{e2}$	$K_{ce}$	$K_1$	$K_2$
2	8	2500	0.03	0.001



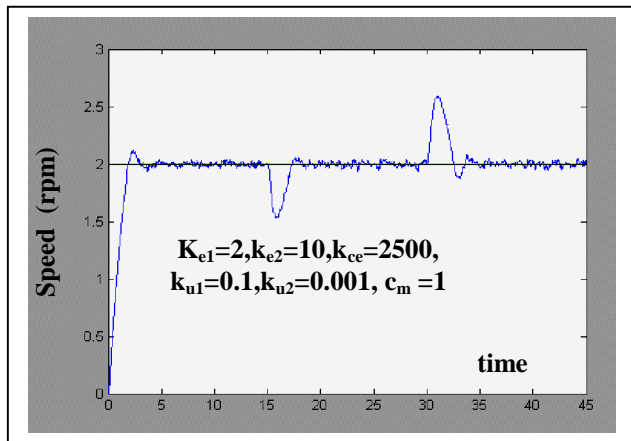


**Fig (26) Response of speed at reference 2000 rpm with load**

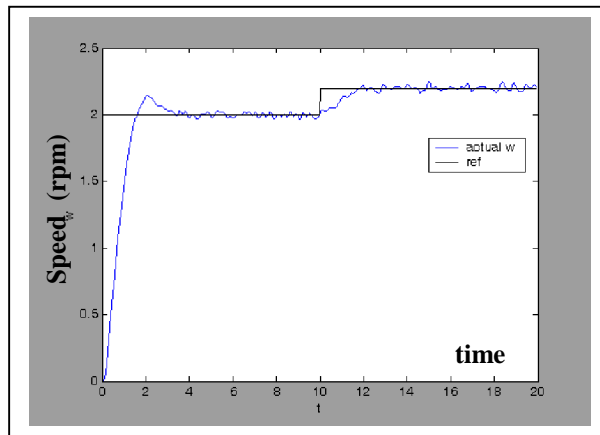


**Fig (27) Response due to reference rpm increase with 10%**

### 6.3 Comparison Between Fuzzy And PID Controllers

In real time simulink, the sample time is set to  $T_s=0.4$  ms with PID controller. But it is increased to 2 ms With fuzzy controller because the fuzzy controller needs a lot of calculations until we get the output signal.

Figure (28) shows the actual speed for system with PID controller and fuzzy controller due to a load increase by 60 % at  $t=15$ sec and decrease to starting value at  $t=30$ sec. The system response with PID controller is smooth without oscillations, while the system with fuzzy controller has fast response with some oscillations. Figure(29) shows the system without load when the the reference speed command decreased by 200 rpm (0.2v), it is clear that the system under fuzzy controller has overshoot and followed the reference speed slowly. It needs to the fuzzy gains must be resetted again in order to obtain a good performance. The system has a good tracking for reference command speed and minimum overshoot.

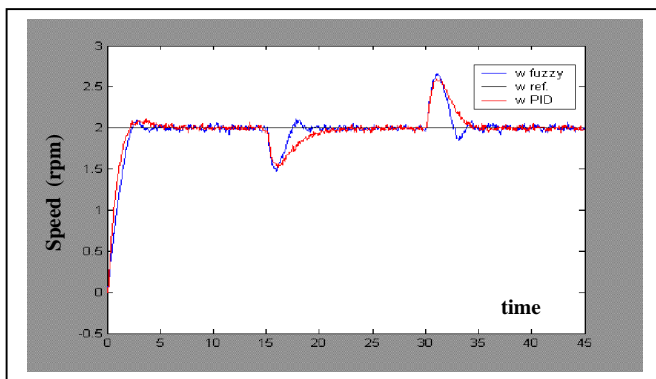


**Fig. 28 Speed response due to load change with fuzzy and PID controller**

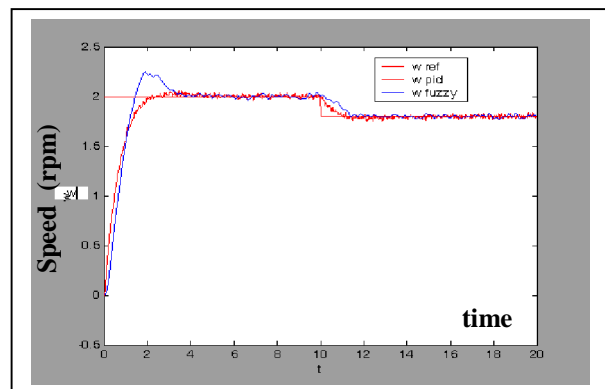


**Fig. 29 Speed response due to reference speed change with fuzzy and PID controller**

## 7. CONCLUSION

The combination of permanent magnet synchronous motor, solid state inverter and rotor position sensor results in a drive system named brushless dc motor having a linear torque-speed characteristics. Motor operation is made self-synchronous by the position sensor that controls the firing signals of the solid state inverter. Fuzzy and PID control techniques can be used to control BLDCM by controlling inverter firing.

The performance of BLDC motor when equipped with PID or fuzzy controllers is tested practically and also using simulation. The practical results agree with simulation results.

The gains of PID or fuzzy controllers are adjusted on line during testing to obtain the best transient response. The starting combination of gains for both PID or fuzzy controllers can be estimated depending on the open loop response and the sampling time that give estimate about the range of error ( $e$ ) and change of error ( $\Delta e$ ) and thus the convenient control action.

It is found that constant gains for the fuzzy controller is not the best choice. Using two values for the error gain ( a smaller value at starting and a greater value near steady state ) improves the response irrespective of small oscillations around the steady state value

## References

- [1] T\_L Chorn and Y\_C Wu “ design of brushless DC position servo system using integral variable structure approach” IEEE proceedings-B, vol. 140, No. 1, PP 27....32, January 1993.
- [2] Pragasen Pillay and Ramu Krishnan “modeling, simulation, and analysis of permanent magnet motor drives, part I, the permanent magnet synchronous motor drives” IEEE transactions on industry applications, vol. 25, No.2 pp 256...273, march/april 1989.
- [3] Pragasen Pillay and Ramu krishnan “modeling, simulation, and analysis of permanent magnet motor drives, part II, the brushless DC motor drives” IEEE transactions on industry applications, vol. 25, No.2 pp 256...273, march/April 1989.
- [4] By Hyeung-Sikchoi, Yong-Heon park, Yongsung Cho, and Minho Lee “Global sliding-mode control” IEEE control system magazine PP 27...35, june 2001.
- [5] Fernando Rodriguez, Aly Emado “A NOVEL DIGITAL CONTROL TECHNIQUE FOR BRUSHLESS DC MOTOR DRIVES” IEEE Transactions on industrial electronics ,Vol,54,No.5,October 2007